

## Evidence for large hydrogen storage capacity in single-walled carbon nanotubes encapsulated by electroplating Pd onto a Pd substrate

A. G. Lipson,<sup>1,2,\*</sup> B. F. Lyakhov,<sup>2</sup> E. I. Saunin,<sup>2</sup> and A. Yu. Tsivadze<sup>2</sup>

<sup>1</sup>Department of Nuclear Plasma and Radiological Engineering, University of Illinois, Urbana, Illinois 61801, USA

<sup>2</sup>A.N. Frumkin Institute of Physical Chemistry and Electrochemistry, Russian Academy of Sciences, 119991, Moscow, Russia

(Received 10 October 2007; published 13 February 2008)

We report a study of hydrogen storage in an alternative material, representing single-walled carbon nanotubes (SWCNTs) encapsulated by thin Pd layers onto a Pd substrate. A synergetic effect resulting in combination of the Pd and the SWCNTs properties with regards to hydrogen has been achieved. Adding SWCNTs increases the H<sub>2</sub> capacity of the Pd-SWCNT composite by up to 25% relative to Pd metal alone under electrochemical loading. This results in a storage capacity of 8–12 wt % with regard to the added SWCNTs.

DOI: [10.1103/PhysRevB.77.081405](https://doi.org/10.1103/PhysRevB.77.081405)

PACS number(s): 81.07.De, 61.46.–w, 61.82.Bg, 68.43.–h

The potential use of single-walled carbon nanotubes (SWCNTs) for effective hydrogen storage<sup>1</sup> has been actively explored during the last decade. Despite previous studies, reporting hydrogen capacity of SWCNT in the range from 0.25 to 20 wt %, <sup>1–9</sup> both reproducibility and reversibility of H<sub>2</sub> storage in SWCNTs still remains poor. Nanotube samples contain impurities, (i.e., amorphous carbon, catalyst, hydrocarbons, water, etc.), which can influence hydrogen adsorption in an uncontrolled manner, leading to large systematic errors. Moreover, a variation in SWCNT diameter and length may affect the hydrogen capacity.<sup>5</sup>

Some authors suggest that the physisorption of hydrogen molecules into the SWCNT must be strictly limited by steric factors representing impurities blocking the SWCNT opening.<sup>6,7</sup> Atomic hydrogen impingement should allow for a better hydrogen uptake due to atomic hydrogen permeation into SWCNT. The result of SWCNTs loading with atomic hydrogen beam was reported by Nikitin *et al.*<sup>9</sup> A 5.5 wt % H<sub>2</sub> gravimetric capacity was achieved with this technique, indicating hydrogen chemisorption into the SWCNT<sup>8,9</sup>.

There is however, another approach to provide massive atomic hydrogen permeation and sorption into the SWCNTs, and this is the topic of the work presented here. Palladium metals possess a unique property to dissociate molecular hydrogen into an atomic form while simultaneously exhibiting high H diffusivity of a quantum character.<sup>10</sup> Thus, if SWCNTs were embedded into a Pd matrix, the result would be an atomic hydrogen or proton flux permeation into the nanotubes under a high pressure of kbar range.

Here we explored a new synergetic approach based upon combining the unique Pd properties (high H-flux diffusivity and pressure) with that of SWCNT (high potential capacity). In searching for high-capacity hydrogen storage, we synthesized a new composite material with the SWCNT encapsulated by thin Pd layers electroplated onto a massive Pd foil to enhance the hydrogen uptake in the SWCNTs. This approach (providing high H<sub>2</sub> pressure from a highly H-loaded massive Pd substrate into a small fraction of deposited SWCNT) allowed us to achieve an additional storage capacity of 8–12 wt % H<sub>2</sub> with regards to the added SWCNTs under electrochemical loading.

Three types of SWCNTs with the same average diameter (1.3 nm), but various lengths, and purity were evaluated: (1)

HiPco™ Bucky™ tubes, lot #79, by Carbon Technologies Inc., (length range 0.5–1.5 μm, purity 95%); (2) SWCNT 7782-42-5, Helix Material Solutions, Inc., (2–20 μm, 90%); and (3) SWCNT Alfa-Aeser (15–40 μm, 95%). The 50-μm-thick cold-rolled Pd foils (Johnson and Mathew, 99.95%), with an area of  $S=1.5–2.0$  cm<sup>2</sup> were used as the substrates. Prior to deposition, the SWCNTs were etched in concentrated nitric acid, for 3 h at  $T=300$  K. The Pd foil preparation is described in Ref. 11. A thin Pd layer of ~0.6 μm thick was electroplated onto the Pd foil (Pd' layer) on both sides from the PdCl<sub>2</sub> electrolyte.<sup>12</sup> The gel of the SWCNT was extracted from the water suspension with  $pH=6.5$ , and applied by dipping the top of the Pd'/Pd/Pd' sample. To encapsulate the SWCNT in the Pd matrix, an additional thin layer of Pd was electroplated on the SWCNTs, coating both sides. The synthesized Pd'/SWCNT/Pd'/Pd/Pd'/SWCNT/Pd' composite foil was subjected to a final annealing in a high vacuum at  $t=500$  °C for 2 h. Similar reference foils of Pd'/Pd/Pd' type were used for comparative analysis of the hydrogen content in the SWCNT.

The interface SEM images of the Pd'/SWCNT/Pd'/Pd/Pd'/SWCNT/Pd' samples are presented in Figs. 1(a) and 1(b). At a lower resolution [ $\times 50\,000$ , Fig. 1(a)] the SWCNT structure appears as aggregates (image appears in the center), surrounded by metallic Pd (image in light color surrounded by SWCNT aggregates). At a higher resolution [ $\times 120\,000$ , Fig. 1(b)] the internal interface between the SWCNT filaments (image in the center) and the electrodeposited Pd coating (site at the edges in gray) are clear and distinctive.

Both the Pd'/SWCNT/Pd'/Pd/Pd'/SWCNT/Pd' (composite) and the Pd'/Pd/Pd' (reference) samples were electrochemically loaded with hydrogen in a special cell with a Pt anode, containing 1 M NaOH solution.<sup>11</sup> The electrolysis was performed at a fixed temperature in a galvanostatic mode at a constant current, with densities ranging from 3 to 30 mA/cm<sup>2</sup> for a period of 0.5–4.0 h. The total electric charge density that passed through the cathode was kept constant at  $Q=45$  C/cm<sup>2</sup>. Immediately after the electrolysis, the samples were transferred into a Dewar glass with liquid nitrogen to prevent spontaneous hydrogen desorption at ambient temperature. Next, the Dewar glass with the sample was

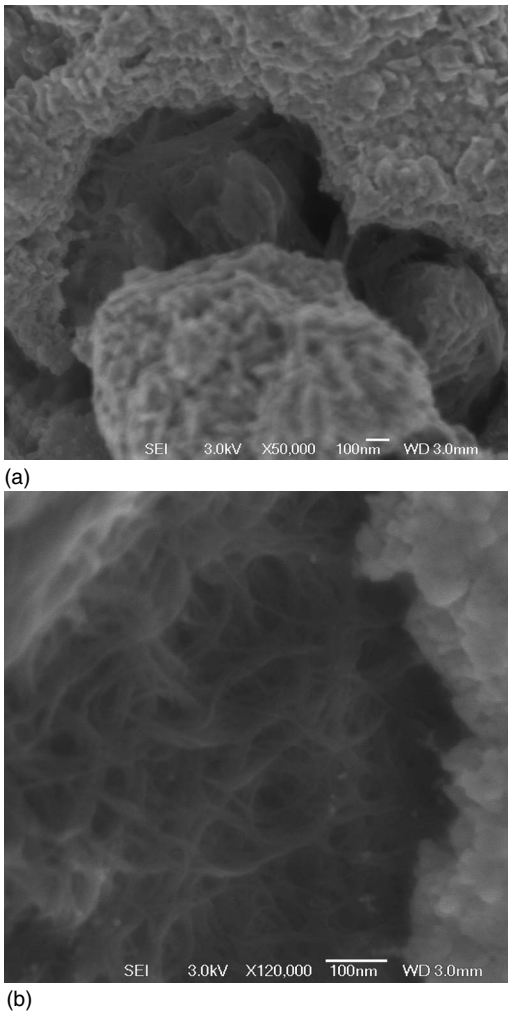


FIG. 1. [(a) and (b)] SEM images of the sites at the Pd-SWCNT interface after 1 min etching in nitric acid: (a) magnification at  $\times 50\,000$  and (b) magnification at  $\times 120\,000$ .

connected to the input of the vacuum desorption apparatus where the samples were rapidly heated to 673 K. The absolute hydrogen concentration in the samples was determined by an isothermic vacuum desorption technique at  $T=673$  K with a residual gas pressure of  $2.0 \times 10^{-6}$  torr. The gas released from the sample transmitted through the hot Pd membrane (serving to separate the hydrogen from other residual gases<sup>13</sup>) and was collected into a closed analytical volume. The pressure was assessed using a three-step mercury McLeod gauge.<sup>14</sup>

The volume of hydrogen in the composite cathodes with etched SWCNT (1), (2), (3)—(Table I, lines 2,4,6) exhibited approximately 20%–25% excess hydrogen, compared to the reference samples (Table I, lines 1,3,5,7). However, there was no excess  $H_2$  found in the composite sample with non-etched SWCNT (1\*) (Table I, line 8), thus indicating an absence of SWCNT loading.

During the five loading-deloaded cycles, the effective loading ratio  $x=[H]/[Pd]$  in the composite sample with SWCNT (1) shows only minor fluctuations resulting in  $\langle x_{\text{eff}} \rangle = 0.86 \pm 0.03$ , while the reference sample (Fig. 2, curve 1) exhibits a constant value of  $\langle x \rangle = 0.68 \pm 0.01$ . Note that the

magnitude of the H/Pd ratio of  $x \leq 0.7$  is normally characterized as the highest Pd loading ( $PdH_x\beta$  phase) that can be achieved electrochemically at a relatively low current density ( $j < 100$  mA/cm<sup>2</sup>) in an alkaline solution.<sup>15,16</sup>

To estimate the gravimetric capacity ( $C_H$ ) of the SWCNT in the composite cathode, we compared the normalized hydrogen volume desorbed from the composite with that from the corresponding reference sample. The net  $C_H$  value was calculated as follows:

$$C_H = 2N_L m_p (V_C - V_0) / M_{\text{SWCNT}}, \quad (1)$$

where  $N_L$  and  $m_p$  are the Loschmidts number and proton mass, respectively;  $V_C$  and  $V_0$  are the  $H_2$  volumes that were desorbed from the composite and the reference sample, respectively; and  $M_{\text{SWCNT}}$  is the SWCNT mass in the composite sample. The net values of  $C_H$  derived from Eq. (1) are shown in Table I (column 6). Remarkably, the  $C_H$  value was higher ( $C_H = 12.0$  wt %) in the shortest SWCNTs (1), whereas the longer SWCNTs (2) and (3) had a lower capacity ( $C_H \leq 8.0$  wt %). In contrast, the original nonetched SWCNT demonstrated no  $H_2$  storage. Thus, we conclude that high loading effect in the SWCNT (1)–(3) is facilitated by the etching process which we believe clears blocked tube openings and allows permeation of the hydrogen atoms inside the SWCNT.

Finally, to be sure that the hydrogen is really stored in SWCNTs we performed  $H_2$  measurement with a higher amount (5.5 mg) of short SWCNTs (type 1a—the same diameter and length as type 1) encapsulated by Pd. As seen from Table I, the net gravimetric capacity for the nanotubes of type 1a (lines 9,10) was found to be the same (within measurement error) as that measured for composites with type 1 nanotubes (lines 1,2). It is also seen that the difference  $\Delta V = 6.54$  cm<sup>3</sup> is larger for higher mass SWCNT-(1a) than that for the lower SWCNT-(1) mass (lines 3 and 4,  $\Delta V = 3.79$  cm<sup>3</sup>), caused by an increase in the amount of  $H_2$  released with a growth of SWCNT mass. Thus, if it is inferred that all of the excess  $H_2$ , beyond the  $x=H/Pd=0.68$  is stored inside the SWCNTs, the storage capacity of the SWCNTs is calculated to be 8–12 wt %.

The kinetics of  $H_2$  escape from the SWCNT (1) at a constant temperature  $T=290$  K are shown in Fig. 3. The reference sample (curve 1), demonstrates only a small reduction in loading  $x=H/Pd$  in the first 15 min (from 0.67 to 0.64). In contrast, the composite sample (curve 2), shows an exponential decay of effective loading, reaching  $x=H/Pd \sim 0.64$  at  $t \geq 60$  min. The activation energy of H desorption at  $T=673$  K derived from the expression  $\exp(-\lambda\tau) = \exp(-\varepsilon_H/k_B T)$ , where  $\lambda$  is the decay constant,  $\tau$  is the duration of H desorption, gives  $\varepsilon_H(\text{Pd}) = 0.20 \pm 0.01$  eV/H atom for the reference, and  $\varepsilon_H(\text{Pd+SWCNT}) = 0.28 \pm 0.01$  eV/H atom for composite samples (inset, Fig. 3). Note that the  $\varepsilon_H(\text{Pd})$  of the reference Pd hydride is in good agreement with that of the hydrogen diffusion in Pd.<sup>10</sup> This fact allows us to extract the activation energy of hydrogen trapping in SWCNT, reasonably assuming that H atoms thermally released from a nanotube, then would diffuse via the Pd matrix and finally escape

TABLE I. Volumetric hydrogen concentration in the Pd'/SWCNT/Pd'/Pd/Pd'/SWCNT/Pd composite and the Pd'/Pd/Pd' reference samples loaded by electrolysis at a constant temperature  $T=290$  K. The samples of Pd'/SWCNT/Pd'/Pd/Pd'/SWCNT/Pd'-(1), (1a), (2), and (3) are synthesized with the SWCNT of types (1), (1a), (2), and (3), respectively. The sample of Pd'/SWCNT/Pd'/Pd/Pd'/SWCNT/Pd'-(1\*) is prepared with nonetched SWCNT of type (1).  $\langle x \rangle = [H]/[Pd] = [2N_L V]/(mN_A/M_A)$ , where  $N_L$  is the Loschmidt number,  $V$  is the desorbed  $H_2$  volume,  $N_A$  is the Avogadro number,  $M_A$  is the atomic weight of Pd, and  $m$  is the Pd mass.  $C_H$  is derived from Eq. (1).

Number	Sample type	Mass (g)	Desorbed $H_2$ volume ( $cm^3$ )	$\langle x \rangle = [H]/[Pd]$	$C_H$ (wt %)
1	Pd'/Pd/Pd'	0.208	$14.61 \pm 0.21$	$0.68 \pm 0.01$	
2	Pd'/SWCNT/Pd'/Pd/Pd'/SWCNT/Pd'-(1), $M(\text{SWCNT})=2.8 \pm 0.2$ mg	0.207	$18.40 \pm 0.32$	$0.86 \pm 0.03$	$12.0 \pm 1.4$
3	Pd'/Pd/Pd'	0.142	$9.83 \pm 0.12$	$0.66 \pm 0.01$	
4	Pd'/SWCNT/Pd'/Pd/Pd'/SWCNT/Pd'-(2), $M(\text{SWCNT})=2.2 \pm 0.2$ mg	0.146	$11.80 \pm 0.20$	$0.79 \pm 0.02$	$8.0 \pm 1.0$
5	Pd'/Pd/Pd'	0.140	$9.80 \pm 0.13$	$0.66 \pm 0.01$	
6	Pd'/SWCNT/Pd'/Pd/Pd'/SWCNT/Pd'-(3), $M(\text{SWCNT})=1.8 \pm 0.1$ mg	0.141	$11.39 \pm 0.23$	$0.78 \pm 0.02$	$7.8 \pm 1.2$
7	Pd'/Pd/Pd'	0.145	$10.13 \pm 0.24$	$0.66 \pm 0.02$	
8	Pd'/SWCNT/Pd'/Pd/Pd'/SWCNT/Pd'-(1*), $M(\text{SWCNT})=1.8 \pm 0.1$ mg	0.148	$10.04 \pm 0.20$	$0.65 \pm 0.02$	0
9	Pd'/Pd/Pd'	0.311	$21.71 \pm 0.39$	$0.66 \pm 0.01$	
10	Pd'/SWCNT/Pd'/Pd/Pd'/SWCNT/Pd'-(1a), $M(\text{SWCNT})=5.5 \pm 0.2$ mg	0.312	$28.25 \pm 0.48$	$0.86 \pm 0.03$	$10.5 \pm 1.5$

the sample:  $\varepsilon_H(\text{SWCNT}) = \varepsilon_H(\text{Pd} + \text{SWCNT}) - \varepsilon_H(\text{Pd}) = 0.08 \pm 0.02$  eV/H atom. The positive difference between activation energies of the composite and the reference samples supports our conclusion that all excess hydrogen in the Pd-SWCNT (compared to containing in the reference Pd sample) is trapped inside the nanotubes.

To check independently the activation energy of hydrogen trapping in SWCNT, we carried out measurements of effective hydrogen loading in the composite and the reference samples in the range of 289–323 K. The H loading into the

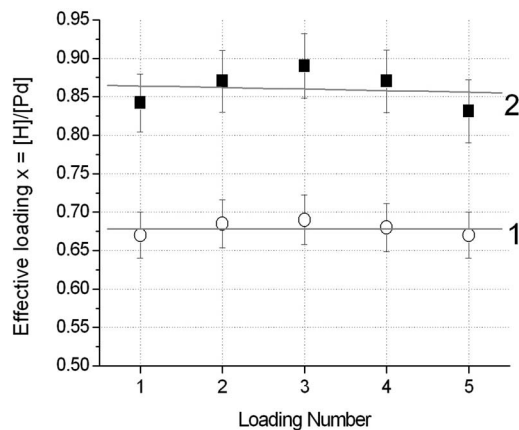


FIG. 2. Hydrogen loading reproducibility for the Pd'/SWCNT/Pd'/Pd/Pd'/SWCNT/Pd' with SWCNT-(1) (curve 2), and for the reference sample of Pd'/Pd/Pd' (curve 1): five consecutive loading-deload cycles. The loading: electrolysis at  $j=5.0$  mA/cm<sup>2</sup> for 2.5 h. The deloading: vacuum heating at  $T=673$  K.

Pd'/Pd/Pd' sample at temperatures above 290 K (Fig. 4) does not appear to be activation dependent (curve 1) because the  $\beta$  phase in PdH<sub>x</sub> cannot thermally decompose below  $T \sim 400$  K.<sup>17</sup> The experimental dependence of the effective hydrogen loading in the composite sample (Fig. 4, curve 2) vs temperature  $T$  can be satisfactorily fitted with a Boltzman sigmoidal function:  $x(T) = a(b-a)\{1 + \exp[(T-T_0)/c]\}^{-1}$ ,

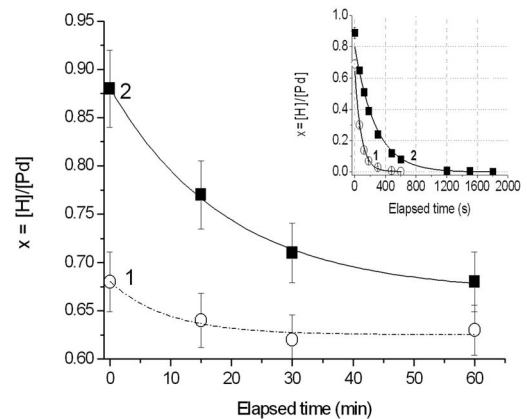


FIG. 3. Effective hydrogen loading in the Pd'/SWCNT/Pd'/Pd/Pd'/SWCNT/Pd' sample with SWCNT-(1) vs time elapsed after completing the electrolysis at  $T=290$  K (curve 2); the same for the reference sample of Pd'/Pd/Pd' (curve 1). Inset: Kinetics of isothermic ( $T=673$  K) degassing for the Pd'/Pd/Pd' (open circles—curve 1): the decay constant  $\lambda(\text{Pd})=0.0087$ , the effective duration  $\tau(\text{Pd})=400$  s, and for the Pd'/SWCNT/Pd'/Pd/Pd'/SWCNT/Pd'-(1) (solid squares—curve 2):  $\lambda(\text{Pd} + \text{SWCNT})=0.004$ ,  $\tau(\text{Pd} + \text{SWCNT})=1200$  s.

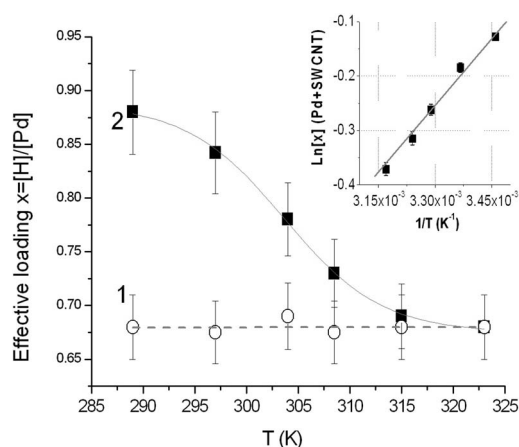


FIG. 4. Effective hydrogen loading in the Pd'/Pd/Pd' (curve 1) and in the composite with the SWCNT-(1) (curve 2) samples vs the loading temperature. The inset shows the Arrhenius plot for the curve 2 data in the coordinates  $(1/T, \text{Ln}[x])$ . The linear fit is consistent with the activation energy of hydrogen absorption  $\varepsilon_{\text{H}} = 0.073 \pm 0.006$  eV/H atom.

where  $a$ ,  $b$ , and  $c$  are the numerical constants, and  $T_0 = 303.65$  K, indicating the stability of hydrogen at  $T \leq 273$  K. The Arrhenius plot of the effective loading  $x(T)$  of the composite cathode is shown in the inset of Fig. 4. The linear fit is consistent with the activation energy of the hydrogen absorption or desorption  $\varepsilon_{\text{H}} = 0.073 \pm 0.006$  eV/H atom, which is close to that estimated from the isothermic desorption data (Fig. 3).

Studies of hydrogen transport and the critical role of Pd substrate in SWCNT loading are underway. Special attention, however, must be given to the fact that the atomic hydrogen generated during permeation through the Pd is

weakly bound in the SWCNT. This effect was not anticipated in the SWCNT without the Pd coating because the interaction of atomic hydrogen with unsaturated C bonds in the SWCNT would result only in chemisorption with a specific energy of  $\varepsilon = 2.5$  eV/H atom.<sup>9</sup> Another possible way to achieve high hydrogen storage,<sup>18,19</sup> involves the formation of a chemical complex at the interface between the transition metal and the nanotube or organic molecules, thus allowing for the absorption of several hydrogen molecules. This is not exactly the case here, because the calculated hydrogen binding energy in the Pd-C complex ( $\varepsilon_{\text{H}} = 0.58$  eV/H<sub>2</sub>) (Ref. 19) would be several times higher than our experimental value. We believe that a possible mechanism of hydrogen adsorption inside the SWCNT could be associated with the formation of a Pd-C complex at the Pd-SWCNT interface due to interaction between the unsaturated C bonds and Pd  $4d$  (hybridized with  $5S$ ) electron shell.<sup>10</sup> This interaction must be accompanied by an electron transfer through the Pd-C potential barrier<sup>20</sup> resulting in a weak polarization of the nanotube's inner wall. In this case, the atomic hydrogen moving through the PdH<sub>x</sub> to the SWCNT openings would permeate the interior of the nanotube, resulting in the formation of a [Pd-C]-H<sub>x</sub> type charge transfer complex. This approach, however, does not give an explanation for surprisingly high storage capacity achieved in our experiments. Further experimental and theoretical works are required to understand the H-storage mechanism in the Pd-SWCNT system.

In summary, we found that electrochemical loading of SWCNTs encapsulated by thin Pd coating results in an additional (compared to pure Pd) storage capacity of 8–12 wt % H<sub>2</sub> with regards to the added SWCNTs. We also demonstrated that hydrogen absorption occurs mainly within the interior of the SWCNT and depends on the SWCNT type.

\*Corresponding author; lipson@uiuc.edu

<sup>1</sup>R. Coontz and B. Hanson, *Science* **305**, 957 (2004).

<sup>2</sup>A. Zuttel, *Mater. Today* **6**, 24 (2003).

<sup>3</sup>M. Becher, C. R. Phys. **4**, 1055 (2003).

<sup>4</sup>F. Lamari Darkrim *et al.*, *Int. J. Hydrogen Energy* **27**, 193 (2002).

<sup>5</sup>A. Zuttel, P. Sudan, P. Mauron, and P. Wenger, *Appl. Phys. A: Mater. Sci. Process.* **78**, 941 (2004).

<sup>6</sup>B. K. Pradhan, A. Harutyunyan, D. Stojkovic *et al.*, *J. Mater. Res.* **17**, 2209 (2002).

<sup>7</sup>C. Matranga and B. Bockrath, *J. Phys. Chem. B* **109**, 9209 (2005).

<sup>8</sup>S. Park *et al.*, *Nano Lett.* **3**, 1273 (2003).

<sup>9</sup>A. Nikitin *et al.*, *Phys. Rev. Lett.* **95**, 225507 (2005).

<sup>10</sup>Y. Fukai and H. Sugimoto, *Adv. Phys.* **32**, 263 (1985).

<sup>11</sup>A. G. Lipson *et al.*, *Phys. Rev. B* **72**, 212507 (2005).

<sup>12</sup>*Modern Electroplating*, 4th ed., edited by M. Schlesinger and M. Paunovic (Wiley, New York, 2000).

<sup>13</sup>V. V. Fedorov *et al.*, *J. Nucl. Mater.* **307-311**, 1498 (2002).

<sup>14</sup>H. P. Hsieh, *Inorganic Membranes for Separation and Reaction* (Elsevier, New York, 1996).

<sup>15</sup>B. Strizker and H. Wuhl, in *Hydrogen in Metals II*, edited by G. Alefeld and J. Volkel, *Topics in Applied Physics Vol. 29* (Springer Verlag, Berlin, 1978).

<sup>16</sup>P. Tripodi *et al.*, *Phys. Lett. A* **276**, 122 (2000).

<sup>17</sup>J. A. Eastman *et al.*, *Phys. Rev. B* **48**, 84 (1993).

<sup>18</sup>T. Yildirim and S. Ciraci, *Phys. Rev. Lett.* **94**, 175501 (2005).

<sup>19</sup>E. Durgun *et al.*, *Phys. Rev. Lett.* **97**, 226102 (2006).

<sup>20</sup>H. Reihert *et al.*, *Phys. Rev. Lett.* **98**, 116101 (2007).